Variations in Thermospheric Neutral Winds and Ionospheric Total Electron Content during January 2013 geomagnetic storm: A comparative study using GOCE Satellite Data, Madrigal FPI and TEC Data, and GITM Simulations

UNIVERSITY OF MICHIGAN

Onyinye G. Nwankwo[1], and Aaron J. Ridley[1]

[1]Department of Climate and Space Sciences and Engineering, University of Michigan, USA

CEDAR 2023

INTRODUCTION

Studying thermospheric neutral winds and ionospheric Total Electron Content (TEC) is key in space weather. Neutral winds, influenced by solar and geomagnetic activity, plus gravitational tides, transport heat and momentum, affecting thermosphere's temperature and density. TEC, a measure of electrons between a satellite and a ground station, reveals the Sun-Earth atmosphere interaction. High TEC during intense solar and geomagnetic activity disrupts Global Navigation Satellite Systems (GNSS) and communication systems.

In January 2013, a geomagnetic storm, a result of coronal mass ejections (CMEs) from the Sun, caused prolonged geomagnetic activity disturbing radio communications, satellite navigation, and visible as auroras at lower latitudes. This event offered a chance to understand solar impact on Earth's magnetosphere, ionosphere, and thermosphere, helping refine space weather models and predictions.

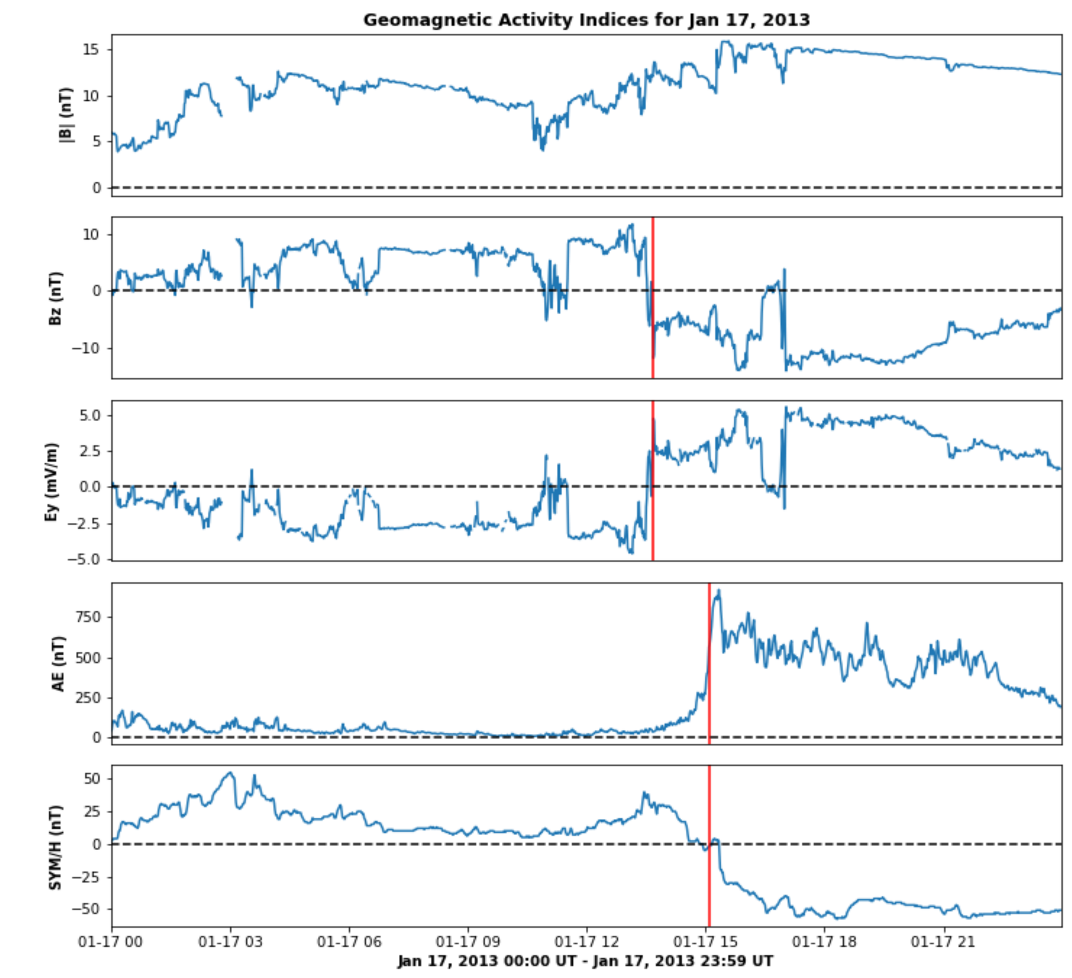

Fig 1: Geomagnetic activity index

PURPOSE OF THE STUDY

The primary objective of this comparative study is to investigate the effects of major factors - specifically viscosity, ion drag, neutral drag, and ion-neutral collision - on the fluctuations in thermospheric neutral winds and the TEC during the January 2013 geomagnetic storm. Another integral part of the study involves exploring the ion-neutral momentum exchange process as detailed in the coupled Navier-Stokes equation. This exchange process serves as a quantitative measure of the ion-neutral coupling strength.

$$\frac{\partial u}{\partial t} + u \cdot \nabla u = -\frac{1}{\rho}\nabla p + \frac{\mu}{\rho}\nabla^2 u + F_{ext} + F_c + F_L$$

Viscosity effects

$F_c \propto v_{in}$; where v_{in} is the ion-neutral collision frequency.

The most impactful in the ionosphere-thermosphere system is the resonant interaction, where, during momentum transfer, electrons can transition from neutrals to ions, subsequently transforming ions into fast neutrals.

Therefore, as the ion drift intensifies, it results in a larger difference between ion and neutral velocities, leading to a more substantial coupling force and increase in electron density. This effect means that the electron density and neutral wind velocity is influenced by ion drift, and the two species (ions and neutrals) start to align in terms of velocity. At the same time, the continuous transition of electrons can lead to an increase in both electron and neutral densities during ion-neutral coupling.

RESEARCH METHODOLOGY

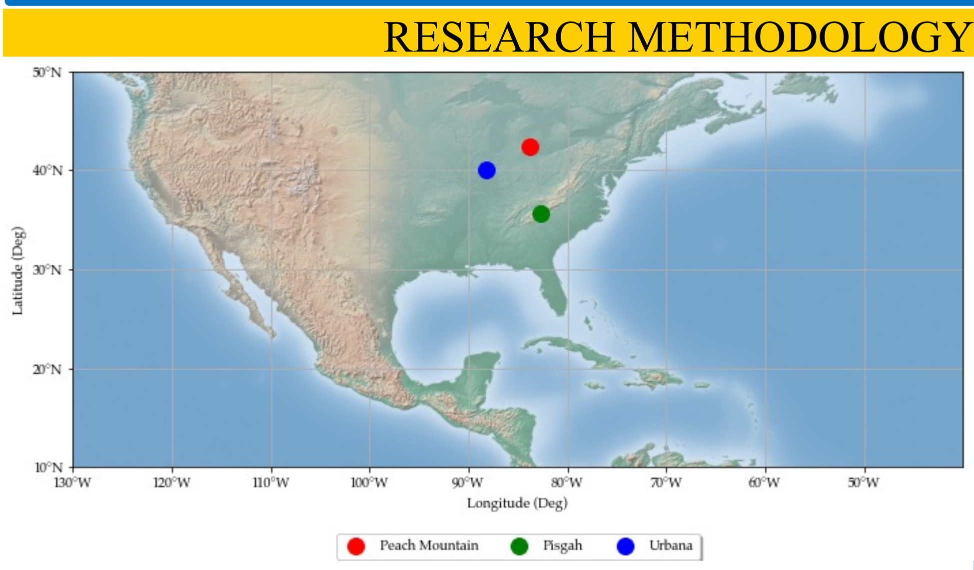

GITM	Run 1 (FTA)	Run 2 (VIS)	Run 3 (v_{in})
Solar Driver	FISM solar EUV flux data	FISM solar EUV flux data	FISM solar EUV flux data
Auroral Driver	Feature Tracking Aurora (FTA) Model	Feature Tracking Aurora (FTA) Model	Feature Tracking Aurora (FTA) Model
Neutral heating efficiency	0.05	0.05	0.05
Eddy diffusion coefficient	50	50	50
Eddy pressure lower	0.010	0.010	0.010
Eddy pressure upper	0.005	0.005	0.005
Thermal conduction (molecular)	5.6×10^{-4}	5.6×10^{-4}	5.6×10^{-4}
Thermal conduction (atomic)	7.6×10^{-4}	7.6×10^{-4}	7.6×10^{-4}
Thermal conduction power	0.72	0.72	0.72
Forcing: Pressure Gradient, Ion drag, Neutral drag, Viscosity, Coriolis, Gravity	TRUE	TRUE	TRUE
Ion Forcing: ExB, Ion Pressure gradient, Ion gravity, Neutral Drag	TRUE	TRUE	TRUE
Improved Ion Advection	TRUE	TRUE	TRUE
Nighttime Ion B. C.s	TRUE	TRUE	TRUE
Viscosity Coefficient	FALSE	TRUE	FALSE
Ion-Neutral Collision frequency Coefficient	FALSE	FALSE	TRUE

1. Zonal wind data were collected from the GOCE satellite during ascending and descending nodes
2. Simultaneously, wind data were collected from ground-based Fabry-Perot Interferometer (FPI) stations at Peach Mountain, Pisgah, and Urbana.
3. Three GITM simulations were executed to study the influence of viscosity and ion-neutral collision frequency coefficients on thermospheric winds and ionospheric TEC during a storm.

PRELIMINARY RESULTS

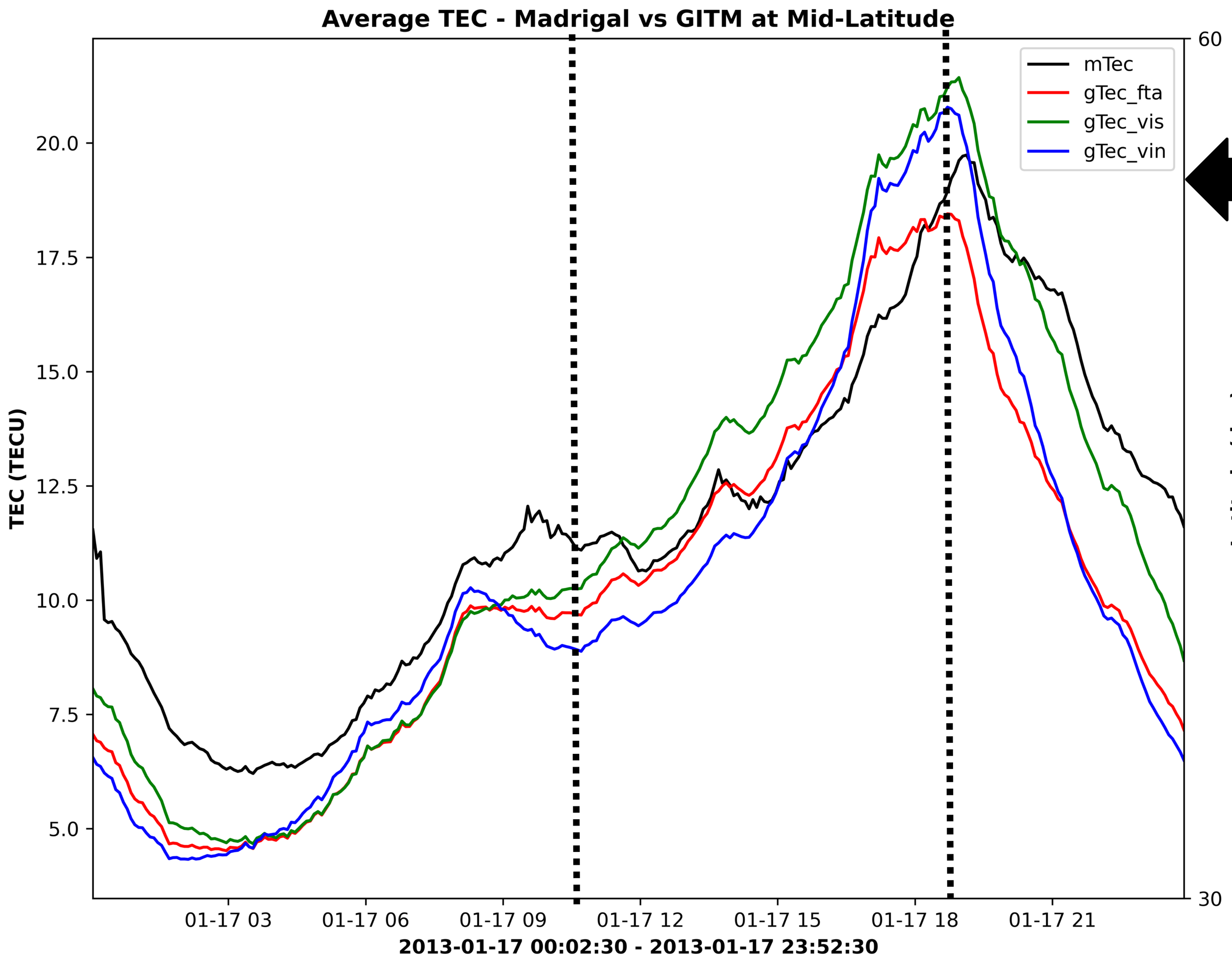

Fig 2: TEC line plot

Figure 2: Average TEC comparison for Midlatitude

- From 00:00 until about 10:00 UT, the mTec demonstrated higher values compared to the three versions of GITM runs.
- The gTec_vis overtook the Madrigal average TEC around 11:00 UT, suggesting the impact of increased viscosity.
- The peak in TEC for both mTec and gTec occurred around 18:15 UT, which aligns with the minimum of the SYM/H index at -58 nT.

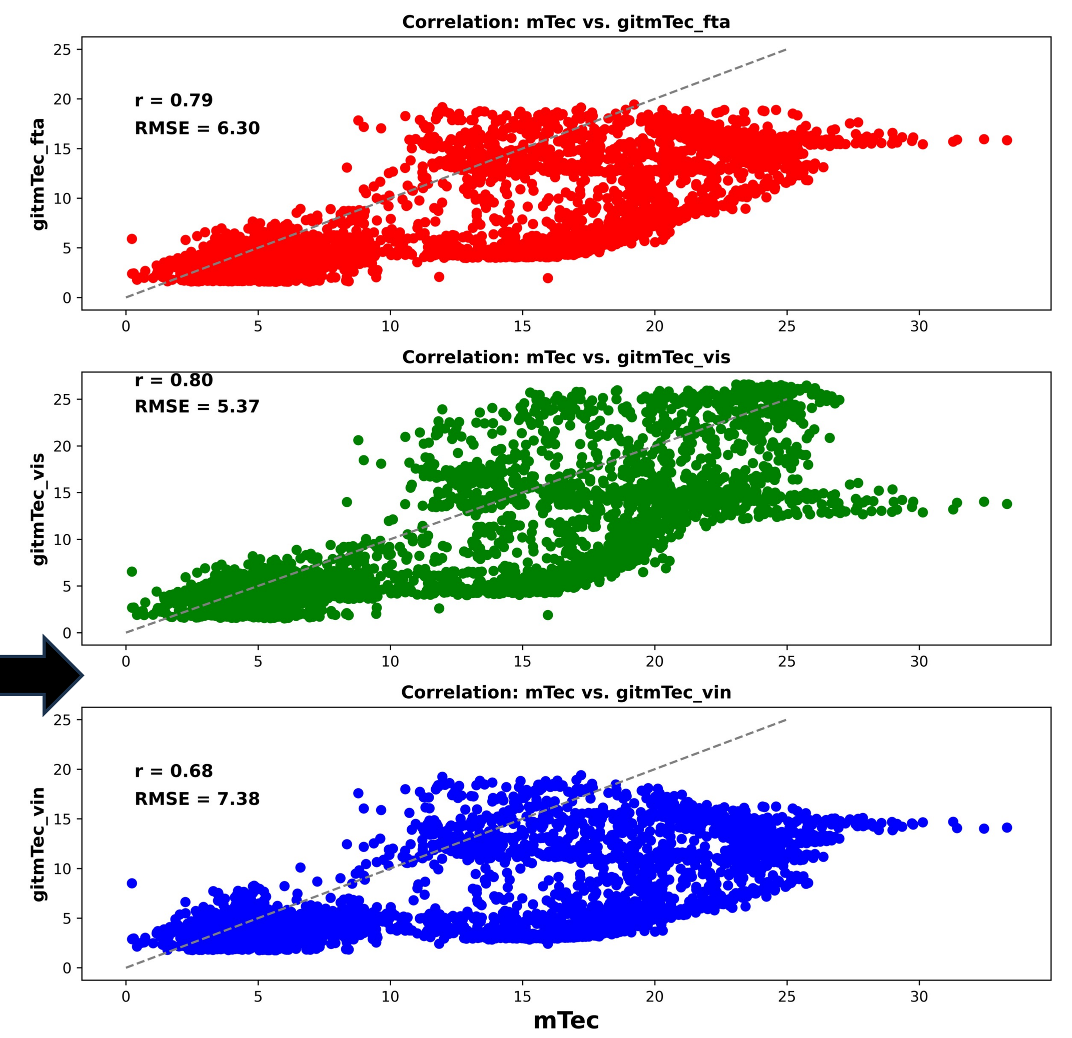

Fig 3: TEC correlation plot

Figure 3: Correlation between mTec and gTec

- gTec_fta demonstrated a strong positive correlation with the mTec. The RMSE value of 6.30 suggests that there might be discrepancies between the gTec_fta simulation results and the observed mTec.
- gTec_vis yielded a slightly stronger positive correlation and a lower RMSE value in comparison to the gTec_fta.
- gTec_vin, despite its consideration of the ion-neutral collision frequency coefficient, exhibited the lowest correlation and the highest RMSE value compared to the other two simulations.

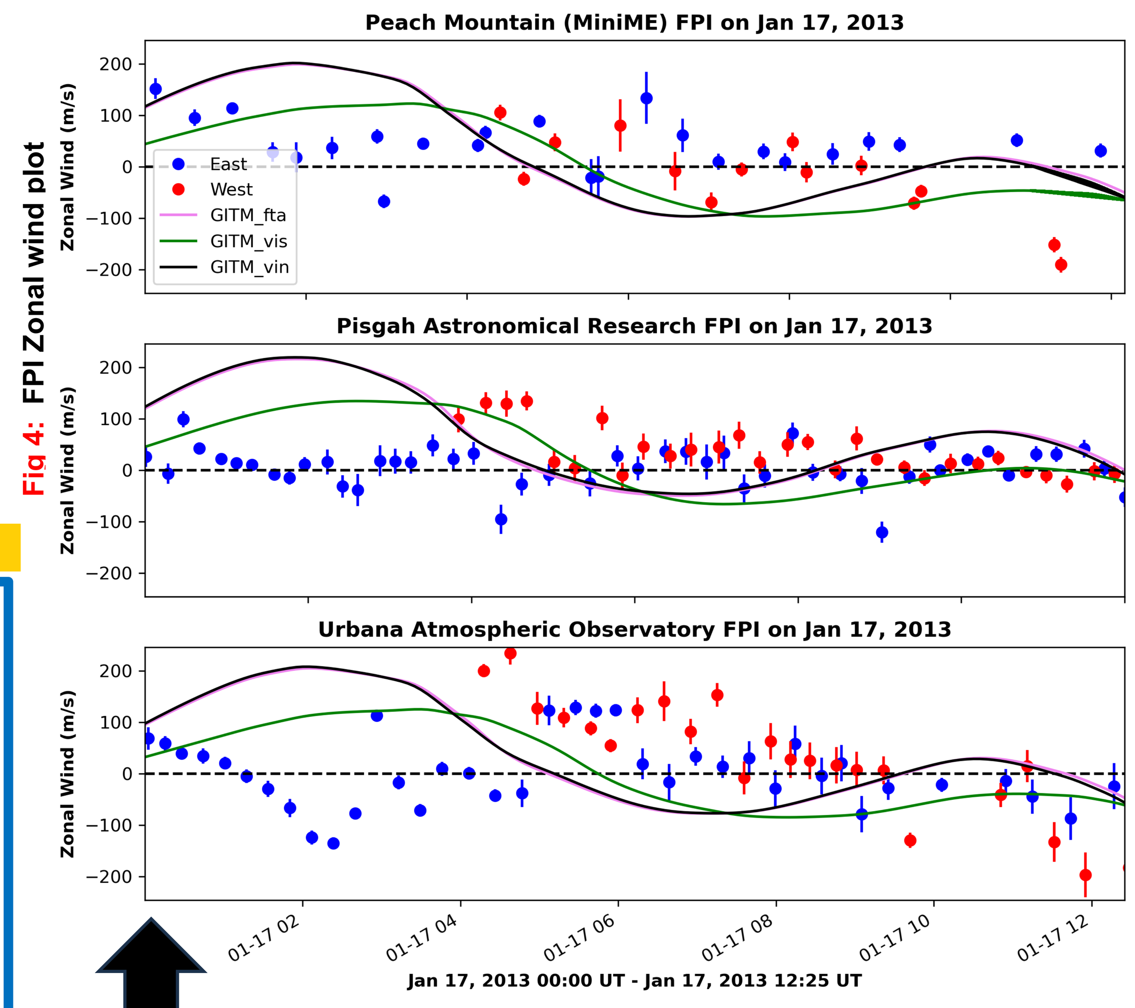

Fig 4: FPI Zonal wind plot

Figure 4: FPI and GITM Zonal Wind comparison

- GITM zonal winds exhibit a to westward flow around 05 UT, and another switch to eastward flow at 09 UT (a phenomenon not captured in the GITM-VIN version).
- One key observation is the enhancement of westward zonal winds, which is triggered by pressure gradients resulting from changes in thermospheric density and temperature.

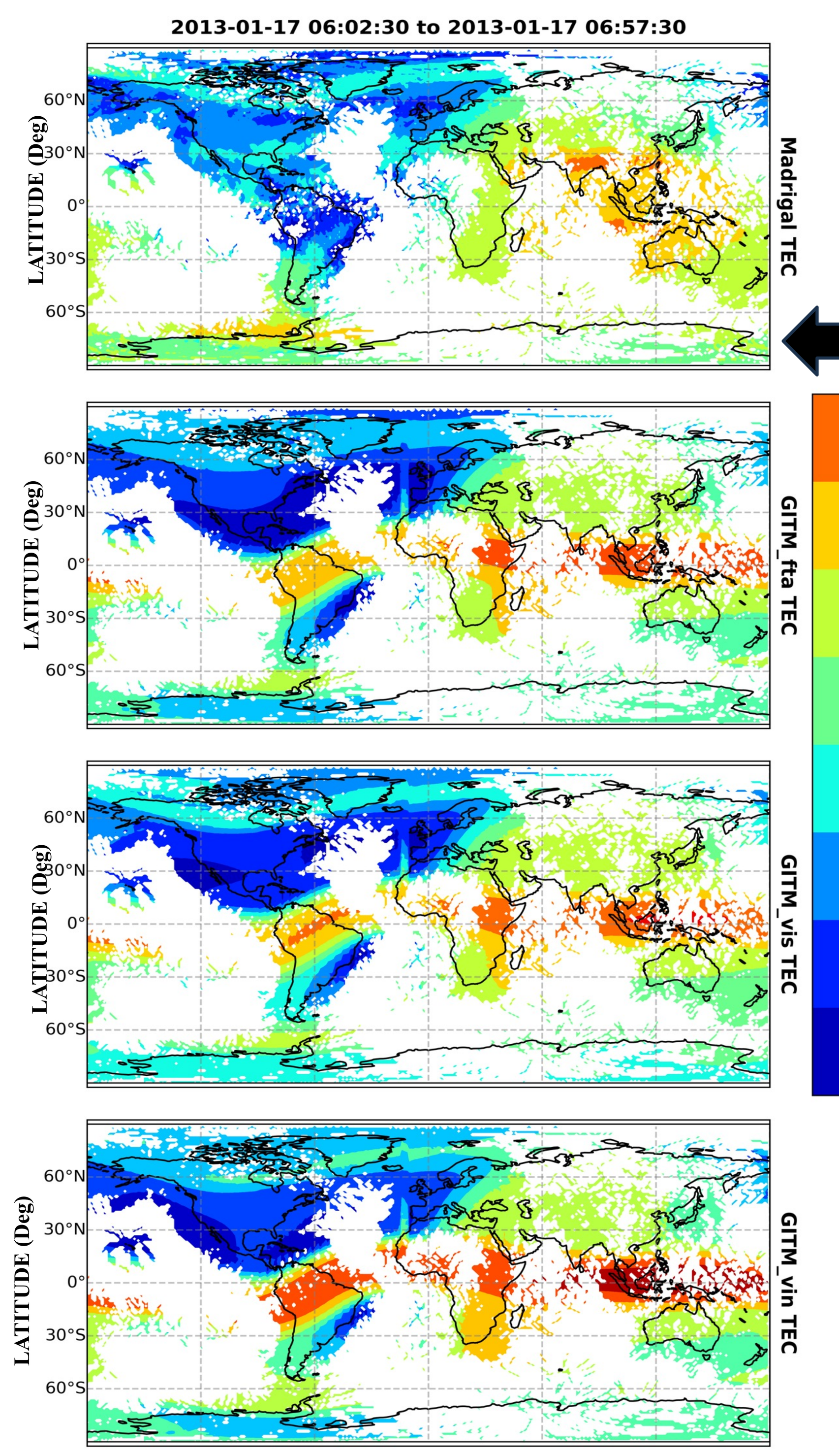

Fig 5: TEC map plot

Figure 5: Madrigal and GITM TEC Map

- The distinct patterns of daytime and nighttime photoionization effects on TEC across mid-latitude North American, European, and Asian sectors can be seen.
- Conversely, in the Asian sector, the effect of daytime photoionization results in increased TEC values.
- The simulations depicted the Equatorial Ionization Anomaly (EIA).

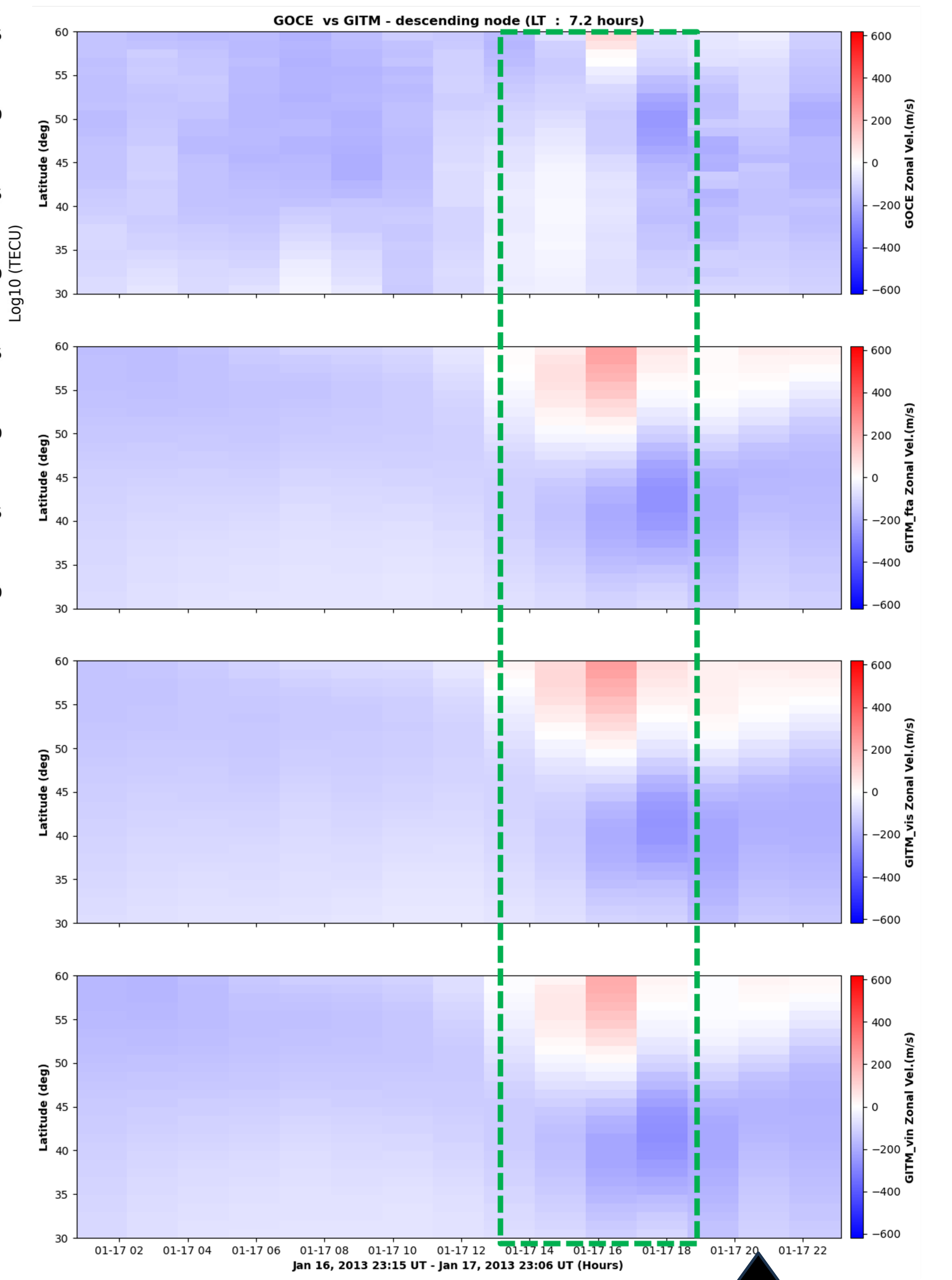

Fig 7: GOCE vs GITM descending node plot

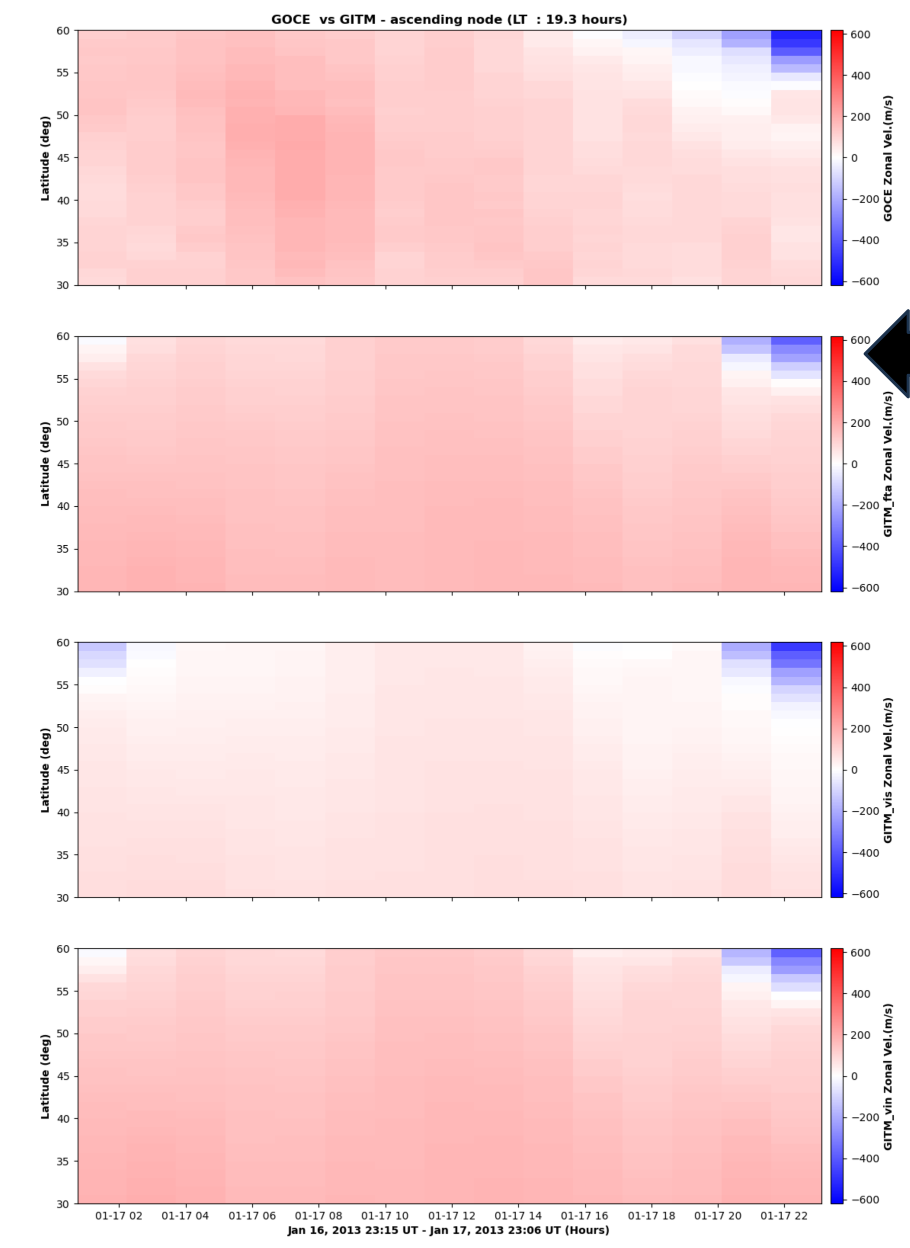

Fig 6: GOCE vs GITM ascending node plot

Figure 6: GOCE and GITM Zonal Wind (Ascending node)

- The comparison between GOCE and GITM simulations during the ascending (near dusk) phase shows all three versions of GITM align with the direction of the GOCE winds in mid-latitude regions. The one exception was seen in the GITM-VIS version, which underestimated the magnitude of zonal wind speed.
- GITM-VIS's underestimation of the wind speed might imply that including viscosity in the model introduces a resistance to motion, counteracting the driving forces in the ionosphere-thermosphere system such as pressure gradients, ion drag, and neutral drag.

Figure 7: GOCE and GITM Zonal Wind (Descending node)

- The descending (near dawn) phase exhibits a change in zonal wind direction at the time when the Bz has its strongest southward turning.
- The southward turning of the Bz can intensify energy input into the night-side magnetosphere and ionosphere, causing increased Joule heating and auroral particle precipitation. These effects circulation changes in the thermosphere, altering the direction and speed of the zonal winds.
- The observed change in the zonal wind direction could be attributed to the alterations in the thermosphere and ionosphere driven by increased energy input into the night-side of Earth and changes in ion-neutral interactions. As a result of increased geomagnetic activity which can also enhance ion drag due to an increased number of ions. This, in turn, can impact the movement of neutral particles, leading to changes in neutral wind direction and speed.

Preliminary Conclusions

- During the main phase of the geomagnetic disturbance, there was a change in zonal wind behavior as seen by GITM simulations and GOCE data, with an emphasis on the descending (near dawn) phase of satellite orbits when the Bz makes a pronounced southward turn.
- The southward shift in Bz intensifies energy input into the ionosphere, triggering an increase in Joule heating and auroral particle precipitation, which leads to significant changes in thermospheric behavior, especially in the direction and speed of zonal winds.
- Concurrently, an increase in geomagnetic activity enhances ion drag due to a rise in the density of electrons and number of ions, affecting the movement of neutral particles and influencing neutral wind direction and speed.

References & Acknowledgement

- Fuller-Rowell, T. J., & Evans, D. S. (1987). Height-integrated Pedersen and Hall conductivity patterns inferred from the TIROS-NOAA satellite data. Journal of Geophysical Research: Space Physics, 92(A7), 7606-7618.
- Ridley, A. J., Deng, Y., & Toth, G. (2006). The global ionosphere–thermosphere model. Journal of Atmospheric and Solar-Terrestrial Physics, 68(8), 839-864.
- Wu, C., Ridley, A. J., DeJong, A. D., & Paxton, L. J. (2021). FTA: A feature tracking empirical model of auroral precipitation. Space Weather, 19(5), e2020SW002629.

The authors would like to acknowledge the operators of the Fabry-Perot Interferometer (FPI) stations and the Madrigal Total Electron Content (TEC) database for making their data available.

nwankwog@umich.edu